Analytical Biochemistry 392 (2009) 1–7

Contents lists available at ScienceDirect

Analytical Biochemistry

journal homepage: www.elsevier.com/locate/yabio

A biotin–hydrogel-coated quartz crystal microbalance biosensor and applications in immunoassay and peptide-displaying cell detection

Hsiu-Mei Chen *, Tsun-Han Huang, Ruey-Ming Tsai

Department of Chemical Engineering, National Taiwan University of Science and Technology, Taipei 10607, Taiwan

ARTICLE INFO

Article history:
Received 2 December 2008
Available online 22 May 2009

Keywords:
Biotin
Hydrogel
Quartz crystal microbalance
Streptavidin

ABSTRACT

A biotin-coated quartz crystal microbalance (QCM) chip was prepared by dip-coating a long-chain alkanethiol-modified crystal with precoupled dextran–biotin hydrogels. The resulting biotin chip was used to affinity-immobilize streptavidin (SAv) and was then further employed for various biosensor assays. First, the SAv chip allowed efficient on-line binding of biotinylated bovine serum albumin (bBSA), followed by a sensitive and specific response toward anti-bovine serum albumin (BSA) antibodies. Three consecutive immunoassays were reproducibly demonstrated with a single chip. The apparent binding kinetics with $k_{on} = 5.9\ \mu M^{-1}\ h^{-1}$, $k_{off} = 10.1\ h^{-1}$, and $K_D = 1.71\ \mu M$ was readily resolved by fitting the real-time sensorgrams. Second, the capability of the SAv chip to selectively recognize recombinant *Escherichia coli* with flagella displaying an artificial SAv binding peptide, *Strep*-tag II, was demonstrated by QCM analysis and verified by scanning transmission electron microscope (STEM) image analysis with biotin-coated gold nanoparticles as the label. Finally, the affinity of the cell-displayed *Strep*-tag II peptide to surface-coated SAv, $K_D = 6.8 \times 10^8$ CFU/ml, was resolved on-line using equilibrium binding kinetics by QCM. This study presents an easy, economical, and reliable method of preparing high-performance SAv-coated biotin chips with potential for application in real-time repetitive immunoassays, on-line binding kinetics studies, and high-affinity peptide screening.

Hydrogel, a three-dimensional insoluble polymeric network that can be homogeneously dispersed in water, is widely investigated and used in modern technology. The gel has high-density capacity due to its flexible and open matrix structure as well as high hydrophilicity, allowing a better accommodation of biomolecules and consequently enhancing biocompatibility, bioactivity, and molecular stability of the gel-fabricated products. Therefore, its successful applications in biotechnology as an entrapping or linking matrix for biomolecules have been reported extensively, in particular in biomedical [1] and biosensing fields over several decades [2–7]. Recently, responsive hydrogels that readily change their physical properties in response to selective biological recognitions have also been studied and show promise in bioapplications [8].

The quartz crystal microbalance (QCM)[1] is a sensitive label-free detector where minute amounts of adsorbed analytes can be readily detected based on the linear relationship between the decreased resonant frequency of a piezoelectric quartz crystal and the mass deposited on its surface [9]. Due to advantages of cost-effectiveness, direct detection, experimental simplicity, fast response, high sensitivity, and real-time output, QCM biosensors have attracted significant interest in biorecognition sensing applications such as DNA detection, immunoassay, molecular interaction studies, and phage screening [10–12]. To better orient and contain more active sensing molecules in a near-native environment, a combination of fabrication techniques consisting of multiple components with different functional roles have been employed to prepare QCM sensing chips. For example, affinity immobilization of biomolecules onto alkanethiol-fabricated gold-coated quartz crystals via ligand-linked hydrogels has been demonstrated as an effective scheme for chip preparation [4,7,13,14] because the multilayer cocoating with long-chain alkanethiols, hydrogels, and affinity ligands can provide combined effects for eliminating undesirable surface denaturation and nonspecific binding and, at the same time, improve chip activity, sensitivity, and stability. Among the selective affinity ligand–target systems, the (strept)avidin–biotin complex is the most popular due to the multivalent and particularly strong interaction. (Strept)Avidin-coated QCM crystals have been developed to directionally and tightly immobilize biotinylated molecules for their subsequent use in selective analyte detection and layer-by-layer assembly fabrication as well as differential recognition of different cell-displayed or

* Corresponding author. Fax: +886 2 2737 6644.
E-mail address: hsiumei@mail.ntust.edu.tw (H.-M. Chen).

[1] *Abbreviations used:* QCM, quartz crystal microbalance; SAv, streptavidin; bBSA, biotinylated bovine serum albumin; BSA, bovine serum albumin; POD, periodate-oxidized dextran; GST/His, glutathione *S*-transferase C-terminally fused with a polyHis tag; 16-MA, 16-mercaptohexadecanoic acid; BAPA, 5-(biotinamido) pentylamine; EDC, 1-ethyl-3-(3-dimethylaminopropyl)carbodiimide hydrochloride; NHS, *N*-hydroxy succinimide; STEM, scanning transmission electron microscope; $NaCNBH_3$, sodium cyanoborohydride.

0003-2697/$ - see front matter © 2009 Elsevier Inc. All rights reserved.
doi:10.1016/j.ab.2009.05.029

phage-displayed biotin-mimic (strept)avidin binding peptides [7,10,13,15,16].

We previously reported an easy affinity preparation of QCM chips hydrogel-coated with streptavidin (SAv) [7]. In that study, hydrogel-coated biotin crystals, which were prepared earlier by incubating alkanethiol-modified crystals in a mixture of derived biotin and oxidized dextran, were used to affinity-immobilize SAv. The performance of such prepared SAv chips in following assays was as satisfactory as that of the other chips prepared by covalently binding SAv. However, because the biotin-coated crystals could maintain good stability under dry storage conditions and be readily used after SAv adsorption, the affinity preparation of SAv chips has the advantage of minimizing the frequency of chip preparation and the variation of coating results over the covalent one. The current article reports an alternative method of preparing hydrogel-coated biotin crystals that saves reagent and is easily quality-controlled. Instead of simultaneously carrying out both conjugation and anchoring reactions, a precoupled dextran–biotin complex was used to fabricate the alkanethiol-modified crystal surface directly. In a flow-through QCM system, the biotin chip was first coated with SAv and then used to immobilize biotinylated bovine serum albumin (bBSA) for a follow-up immunoassay as well as to detect recombinant *Escherichia coli* cells with flagella displaying an artificial SAv binding peptide. Further studies on repetitive usability and specificity of the bBSA-coated chips and on binding kinetics demonstrated the application potential of the prepared biotin chips for bioassays.

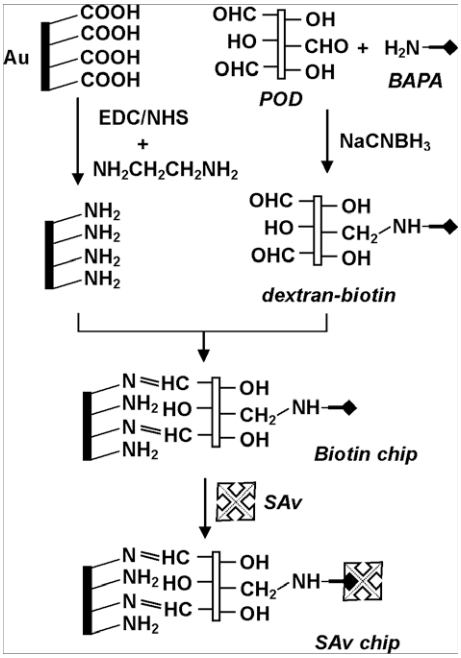

Fig. 1. Schematics of crystal surface fabrication. A carboxyl-terminated crystal prepared by 16-MA coating was modified with EDC/NHS and then ethylenediamine to have amino termini prior to the linking with the dextran–biotin complex. The yielded biotin chip was then used to immobilize SAv through affinity interaction.

Materials and methods

Materials

Gold-deposited QCM crystals (9 MHz) and periodate-oxidized dextran (POD, derived from dextran of molecular weight ~ 70,000) were prepared as reported previously [3,7]. Two different *E. coli* GI826 cells carrying pFliTrx and pStrepII, respectively, were constructed earlier in our laboratory [7]. Recombinant *Schistosoma japonicum* glutathione *S*-transferase C-terminally fused with a polyHis tag (GST/His) was produced and affinity-purified as described previously [17]. 16-Mercaptohexadecanoic acid (16-MA, $HS(CH_2)_{15}COOH$) and monoclonal mouse antibody against polyHis were purchased from Sigma–Aldrich (St. Louis, MO, USA). Native SAv was obtained from Zymed Laboratories (San Francisco, CA, USA). bBSA and 5-(biotinamido) pentylamine (BAPA) were obtained from Pierce Biotechnology (Rockford, IL, USA). Polyclonal sheep antibody against BSA was purchased from The Binding Site (Birmingham, UK). In addition, 1-ethyl-3-(3-dimethylaminopropyl)carbodiimide hydrochloride (EDC) and *N*-hydroxy succinimide (NHS) were obtained from Wako Pure Chemicals Industries (Osaka, Japan). Scanning transmission electron microscope (STEM) Formvar/Carbon grids (200 mesh, cat. no. FCF200-Cu) were obtained from Electron Microscopy Sciences (Hatfield, PA, USA). Gold nanoparticles (20 nm) were purchased from NanoTake Technology (Taipei, Taiwan).

Chip preparation

The preparation procedure of biotin chips and SAv chips is illustrated in Fig. 1. A dextran–biotin complex was prepared prior to surface fabrication. For this, POD (0.02% [w/v] in 0.1 M phosphate buffer, pH 6.0) was reacted with an excess amount of BAPA at pH 6.0 and 4 °C for 72 h. After reducing the Schiff's bases formed between POD and BAPA with sodium cyanoborohydride ($NaCNBH_3$), the dextran–biotin complex solution was dialyzed against deionized water and then stored at 4 °C for further use.

To prepare biotin chips, gold-deposited QCM crystals were first treated with 3 mM 16-MA at room temperature for 2 days, activated with 0.2 M EDC/NHS at 30 °C for 2.5 h, and then modified with 0.05 M ethylenediamine at 30 °C for 2 h. After blocking unreacted active sites with 0.1 M ethanolamine at room temperature for 1 h, the amine-terminated crystals were dip-coated with the dextran–biotin solution at 4 °C overnight, rinsed with phosphate buffer (10 mM, pH 7.2) and then deionized water, and finally stored dry at 4 °C. For SAv coating, a biotin chip was either immersed in a static solution of 15 μM SAv in 10 mM phosphate buffer (pH 7.2) at 4 °C for 3 h or flowed over with 3.7 ml of 1.5 μM SAv in a flow-through QCM detection system described below.

Biosensor measurement

The detection system was set up as described previously [3]. A QCM analyzer with 1 Hz resolution with an oscillating circuit and a frequency counter (Smart Biotechnology, Taipei, Taiwan) was connected to a QCM crystal via an extended oscillating unit and to a PC workstation for data acquisition. The crystal was placed inside a thin-layer flow-through cell (internal volume = 34 μl, diameter = 5 mm), which was sequentially connected to working and regeneration buffer tanks, a sample injector in the upstream, and a peristaltic pump in the downstream to control the flow rate. The system was run at room temperature and with a specified flow rate with acetic buffer (5 mM, pH 5.0) as the working solution, and the frequency data were collected at 1-s intervals. For BSA immunoassay, an SAv-coated chip was first flowed over with 2 ml of 1.4 μM bBSA, rinsed with the working buffer until the resonant frequency reached a steady value, and then injected with 2 ml of 0.3 μM anti-BSA antibody. To regenerate the bBSA-coated chip for repetitive detection of antibodies, the chip was washed with 5 ml of 0.1 M glycine–HCl buffer (pH 2.3) to dissociate the antigen–antibody complex and then reequilibrated with the working buffer. For peptide-displaying *E. coli* cells, the cell cultivation and the QCM detection were carried out as described previously [7],

with an additional infusion of glycine–HCl between each cell injection to regenerate the sensing chip.

For sensorgram analysis, the equilibrium frequency shift ($-\Delta F_e$) is defined as the decrease of resonant frequency from the beginning of an analyte injection to the final steady state achieved after rinsing with the working buffer. To mathematically resolve the adsorption sensorgrams resulting from continuous injection of analytes over a sensing chip, Eq. (1) was used [10]:

$$\Delta F = \frac{\Delta F_{\max,on} k_{on} C}{k_{on} C + k_{off}} \times \left[1 - e^{-(k_{on} C + k_{off}) \times (t - t_0)}\right], \quad (1)$$

where ΔF is the frequency shift, $\Delta F_{\max,on}$ is the fitted maximum shift on complete coverage, C is the molar concentration of analyte, k_{on} and k_{off} are the apparent association and dissociation rate constants in the current flow system, respectively, and t_0 is the time at start of adsorption. To depict desorption, where the adsorbed analytes were dissociated from the chip surface with a continuous flow of working buffer, Eq. (2) was employed to fit the sensorgram:

$$\Delta F = \Delta F_{\max,off} \times \left[1 - e^{-k_{off} \times (t - t_0)}\right]. \quad (2)$$

STEM analysis

Prior to the imaging, gold nanoparticles were sequentially treated with 16-MA, activated with EDC/NHS, modified with ethylenediamine, and finally coated with dextran–biotin following the procedure for the preparation of biotin chips, as described earlier. Meanwhile, the cells to be examined (1 ml, 9×10^6 CFU/ml) were incubated with 0.1 ml of 15 μM SAv at pH 7.2 and 25 °C for 1 h, collected with centrifugation, and resuspended with 1 ml of sterile water in sequence. For imaging, 5 μl of the SAv-treated cells were reacted with the biotin-coated nanoparticles (0.5 ml, 37.5 μM) for 6 h, and then 20 μl of the mixture was subjected to STEM analysis using a JEOL JEM-2000FX STEM operating at 140 kV.

Results and discussion

Preparation of biotin chips

When preparing the dextran–biotin complex, ninhydrin tests were constantly carried out to confirm the coupling of BAPA to POD. A much less intense blue–purple color was obtained from the BAPA and POD mixture than from the equivalent BAPA solution, indicating that the amine termini of BAPA molecules had been consumed through the Schiff's base linkages with POD.

Following the procedure depicted in Fig. 1, the Schiff's bases in the complex were further reduced with a mild but highly specific reagent, $NaCNBH_3$, to ensure the stability of the dextran–biotin linkages in long-term storage, multiple uses, and continuous-flow biosensor assays as well as to maintain the reactivity of the residual aldehydes on POD. The dextran–biotin complex was subsequently attached to a prefabricated amine-terminated QCM crystal via these residual aldehyde groups to yield a biotin chip and finally an SAv chip by affinity immobilization. The Schiff's base linkages formed between POD and surface amines were left unreduced because the QCM responses in our previous studies consistently showed that the bulky POD matrix linked by unreduced Schiff's bases remained stably attached to the crystal surface throughout each flow-through assay [3,4,7,14]. This might be due to multiple attachments of each POD molecule onto the surface and the possibility that the insoluble polymeric network of POD hydrogel could hinder the susceptibility of surface Schiff's bases to hydrolysis. Table 1 shows the frequency shift values of the fabricated crystals, confirming the successful coating of each layer.

Table 1
Immobilization of biotin and SAv onto gold electrodes of QCM crystals.

Fabrication step	Frequency shift[a] ($-\Delta F$, Hz)	Deposited mass[b] (ΔM, μg)
16-MA	872 ± 248	1.11
Modification[c]	221 ± 76	0.28
Dextran–biotin	102 ± 39	0.13
SAv	156 ± 46	0.20

[a] Values are reported as averages of 8 crystals ± standard deviations. The resonant frequencies were measured after the treated crystals had dried.
[b] Estimated by a theoretic sensitivity of 784 Hz/μg in the air, which was derived from the Sauerbrey equation [9].
[c] Modification included the EDC/NHS activation, ethylenediamine modification, and ethanolamine blocking steps.

QCM immunoassay

Throughout this study, a low-ionic and mildly acidic solution, 5 mM acetic buffer at pH 5.0, was used as the working buffer for all flow-through QCM analyses because it yielded a better binding when flowing bBSA over SAv chips than other buffers near physiological pH, as shown in our previous study [7]. Unlike static coating, where satisfactory results were readily achieved under physiological conditions, a mildly acidic environment was required for flow coating. This may be due to the decrease of binding affinity caused by continuous shear flow, raising the need to maintain SAv near its isoelectric point (pH 5.0) so as to achieve the maximum stability and the minimal dissociation rate constant for the SAv–biotin complex [18]. Therefore, for experimental simplicity and to ensure the maintenance of stable SAv–bBSA constructs during the flow assays, this acetic buffer was also used as the working buffer in immunoassays. Despite the fact that this is not the optimal condition for antigen–antibody interaction, detectable immunoassay results have been reported before [19,20]. As for hydrogel stability, the possibility of gel stripping caused by acid-catalyzed hydrolysis of Schiff's base linkages between POD and surface amines can be excluded because no significant increase of the resonant frequency beyond the initial value was observed in our QCM sensorgrams, as shown below.

Fig. 2 demonstrates the on-line coating of bBSA and subsequent immunoassay of anti-BSA with a single biotin chip. The biotin chip was subjected to consecutive injections of SAv, bBSA, and anti-BSA, with intermittent rinsing with the working buffer between two samples. The fresh working buffer was injected with the intent to

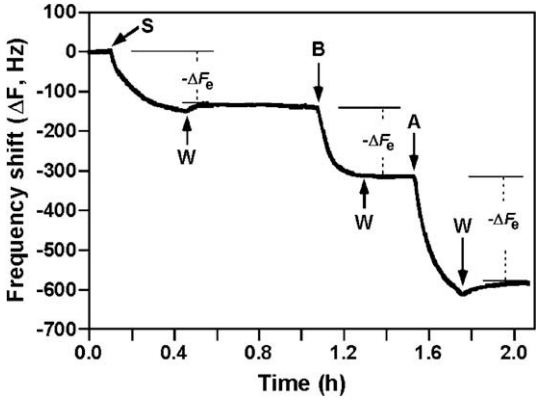

Fig. 2. Real-time sensorgram of immunoassay of anti-BSA with a biotin chip. S, 1.5 μM SAv; W, working buffer; B, 1.4 μM bBSA; A, 0.3 μM anti-BSA. Flow rate: 180 μl/min. The $-\Delta F_e$ value for each analyte injection cycle was determined as shown in the figure.

disrupt the interaction between the bound analytes and the surface-capturing molecules to yield a dissociation sensorgram. As shown in Fig. 2, the injection of each analyte caused the crystal frequency to decline promptly with a considerable amount of shift, suggesting the high sensitivity and fast response of this detection system and its applicability for continuous on-line coating and assays. The follow-up rinsing resulted in only very slight dissociations of SAv and anti-BSA from the chip surface, but no dissociation of bBSA was observed, implying that the interaction between the captured bBSA and the chip surface SAv was the strongest among the three studied analyte–ligand pairs. Insignificant on-line dissociation of bBSA from the SAv-coated surface was also observed in our previous study for both affinity-prepared and covalently prepared SAv chips [7].

The data analysis of Fig. 2 is summarized in Table 2. By considering the molecular weights of bBSA, SAv, and anti-BSA as 69.5, 66, and 150 kDa, respectively, the molar ratio of bound analytes to surface-capturing molecules in each injection cycle could be estimated based on their respective $-\Delta F_e$ values. For the bBSA injection cycle, the molar ratio of bound bBSA to surface SAv was determined as 1.25, a value corresponding to saturation coverage of bBSA over the SAv surface due to the fact that the crystal had reached a steady resonant frequency before being rinsed with the working buffer. Because SAv is a tetravalent biotin binding protein and at least one of its binding sites should have been used for anchoring on the biotin chip, the theoretical number of maximum residual binding sites remaining available on each surface SAv to capture flowing bBSA was 3. Therefore, our estimated value of 1.25 suggests that the three-dimensional porous network structure of the hydrogel in this study enabled each surface SAv to freely bind with more than one bBSA molecule. However, the theoretical value of 3 could not be achieved because of the steric hindrance interaction of the bulky bound bBSA molecules. As for the anti-BSA cycle, the molar ratio of bound anti-BSA to surface bBSA was estimated as 0.71. As observed in Fig. 2, the adsorption sensorgram of anti-BSA was still declining when the working buffer was injected. Therefore, a higher molar ratio could be expected if a sufficient amount of antibodies was injected to fully saturate the bBSA molecules in the hydrogel matrix.

Immunoassay kinetics

The sensorgrams of each injection cycle in Fig. 2 were analyzed by nonlinear regression to investigate the apparent binding affinity of each bound analyte to its respective surface-capturing molecules. As shown in Fig. 3, except for the desorption sensorgram of bBSA where no noteworthy frequency retrieval was observed, all of the other adsorption and desorption sensorgrams were satisfactorily fitted with Eqs. (1) and (2), respectively, with the regression parameters shown in Table 2. The k_{off} and $k_{on}C + k_{off}$ values of SAv and bBSA injections were similar to those obtained in our previous study [7], where the biotin chips were prepared simply by immersing amine-terminated crystals into a mixture and BAPA and POD and where the same injectant concentrations as in this study were used. This suggests the similar structures of both biotin hydrogels in the current and previous studies and the consistency of these two QCM biosensor studies.

For the SAv injection cycle, the regression value of k_{off} obtained using Eq. (2) was higher than that of $k_{on}C + k_{off}$ obtained using Eq. (1), so the attempt to estimate the k_{on} value for SAv binding was not achieved. This inconsistency might arise from the possibility

Table 2
Analysis of the immunoassay sensorgram of a biotin chip.

Injectant	SAv	bBSA	Anti-BSA
$-\Delta F_e$ (Hz)	134	177	272
$-\Delta F_{max,on}k_{on}C$[a] (Hz h^{-1})	1467 ± 5[b]	3145 ± 13	3704 ± 8
$k_{on}C + k_{off}$[a] (h^{-1})	9.3 ± 0.0	17.7 ± 0.1	12.0 ± 0.0
$\Delta F_{max,off}$[c] (Hz)	18.6 ± 0.0	—[d]	29.5 ± 0.1
k_{off}[c] (h^{-1})	32.8 ± 0.6	—[d]	10.1 ± 0.1
k_{on}[e] ($\times 10^6$ M^{-1} h^{-1})	ND[f]	ND[f]	5.9
K_D[g] (μM)	ND[f]	ND[f]	1.71

Note. Data originated from Fig. 2.
[a] Estimated by fitting the association sensorgrams using Eq. (1) as shown in Fig. 3.
[b] Standard errors derived from the fitting process.
[c] Estimated by fitting the dissociation sensorgrams using Eq. (2) as shown in Fig. 3.
[d] Not fitted due to no frequency retrieval.
[e] Estimated according to the resulting fitting values of k_{off} and $k_{on}C + k_{off}$.
[f] Not determined due to either the fact that k_{off} is larger than $k_{on}C + k_{off}$ for the SAv injection or insufficient fitting data for the bBSA injection.
[g] Determined from k_{off}/k_{on}.

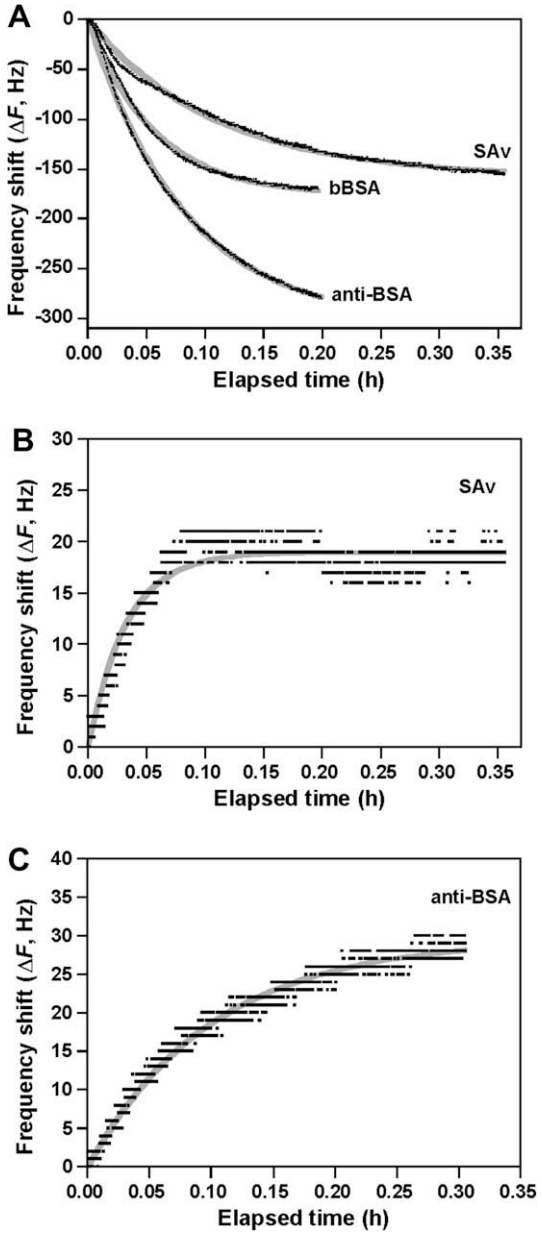

Fig. 3. Kinetic analysis of the sensorgram of Fig. 2. (A) Curve-fitting the SAv, bBSA, and anti-BSA association sensorgrams using Eq. (1). (B, C) Curve-fitting the SAv (B) and anti-BSA (C) dissociation sensorgrams, respectively, using Eq. (2). The gray solid lines represent the regression curves.

of different apparent k_{off} values between the adsorption and desorption phases. In adsorption, the continuous infusion of fresh SAv could force SAv to rebind onto the chip surface, yielding a smaller apparent k_{off} value than that in the desorption phase. Such a rebinding phenomenon might be less significant in the anti-BSA association phase, possibly because of its larger size, so the apparent k_{on} value of the anti-BSA injection cycle, as well as the apparent K_D value, could be readily estimated. The estimated K_D value (1.71 μM) is somewhat larger than those values obtained for the binding of flowing anti-BSA toward non-hydrogel- and hydrogel-immobilized BSA using surface plasmon resonance (0.84 and 0.13–0.19 μM, respectively) [21,22]. The lower affinity observed in this study may be caused by hindrance from the 7 or 8 biotin molecules conjugated on each BSA and the mild acidity of the working buffer used in the binding assay. For future immunoassay applications, modified avidin or recombinant SAv with near-neutral isoelectric points may be used instead of native SAv so that a working buffer at physiological pH can be employed to increase the binding affinity.

Selectivity and repeatability of bBSA chips

Fig. 4 shows the frequency response of an SAv chip on consecutive injections of bBSA, GST/His, and anti-BSA. GST/His was used to check the selectivity of the chip, and the glycine–HCl buffer was injected to disrupt any protein–protein interaction for chip regeneration. As is usually observed with this detection system [3], the glycine–HCl infusion caused the frequency to drop sharply downward and fluctuate vigorously. The frequency of the bBSA-coated chip responded to the injection of a high concentration of GST/His (10 μM) with a very small and slow decline that could be completely retrieved after rinsing with the working buffer. On the other hand, a distinct and rapid decrease with minor restoration was once again observed when the same chip was reinjected with a 0.3-μM anti-BSA solution that was much more dilute than GST/His. Another study with the injection of antibodies against polyHis tags over a bBSA-coated chip also resulted in a poor response similar to that of GST/His (data not shown), suggesting the high selectivity of the prepared chip.

Fig. 5 shows the frequency response of an SAv chip on bBSA coating and three subsequent consecutive injections of anti-BSA. The repetitive profile demonstrates the feasibility of continuous real-time assays of multiple anti-BSA samples using a single on-line coated bBSA chip. The frequency was almost completely retrieved after each glycine–HCl regeneration, indicating that the bound anti-BSA molecules had been entirely dissociated from the chip surface. The first infusion of the acidic buffer might have also caused some degree of irreversible denaturation of bound bBSA, especially for the molecules with less stable initial conformation; thus, the frequency responses to the antibody injections declined to nearly constant levels in the next two consecutive cycles. Nevertheless, the acid regeneration process did not result in any removal of surface-bound bBSA antigens from the SAv chip surface, as observed in our previous study [7]. This suggests that the strong interaction between SAv and biotin provides a highly reliable technique of immobilizing biomolecules on biosensor surface for continuous, repetitive, and single-chip on-line assays.

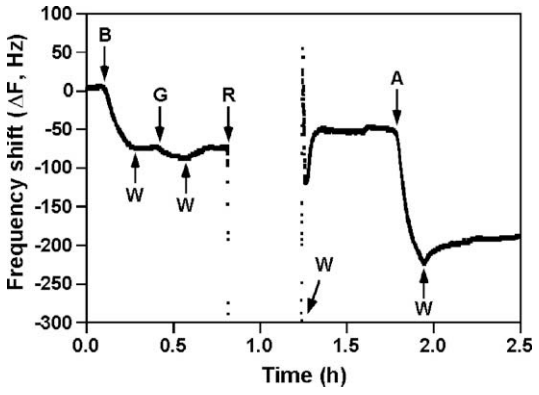

Fig. 4. Differential responses of an SAv chip toward GST/His and anti-BSA after on-line coating with bBSA. SAv was adsorbed onto the biotin chip by the static immersion method. The descriptions of A, B, and W are the same as those in Fig. 2. G, 10 μM GST/His; R, glycine–HCl buffer. Flow rate: 205 μl/min.

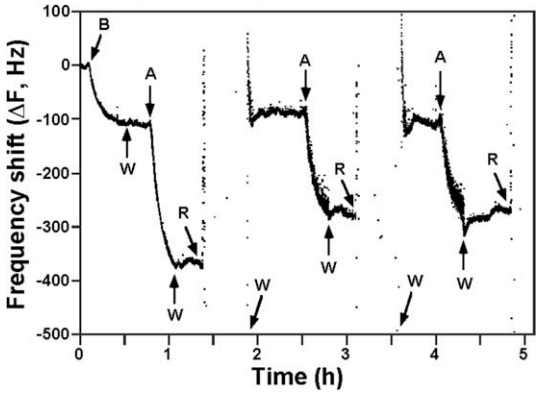

Fig. 5. Continuously repetitive detection of anti-BSA with a single SAv chip after on-line coating with bBSA. SAv was adsorbed onto the biotin chip by the static immersion method. The descriptions of A, B, R, and W are the same as those in Figs. 2 and 4. Flow rate: 180 μl/min.

QCM assays of peptide-displaying cells

The flagellum display random peptide library, where diverse peptides are cloned and displayed on *E. coli* flagellum surface by means of a flagellin–thioredoxin fusion construct using pFliTrx as the expression vector, is a useful tool to screen functional peptides for drug discovery, protein–protein interactions, and biotechnological applications [23]. With the advantages of real-time assay and availability of automation, high-throughput, and direct investigation of binding kinetics, biosensors have been considered as a valuable auxiliary device for library screening. In the current study, to demonstrate the feasibility of using the prepared biosensor to selectively detect and analyze functional peptides from a flagellum display library, an artificial SAv binding peptide that was previously selected through random peptide libraries [24], *Strep*-tag II, was cloned in a pStrepII plasmid, expressed on *E. coli* GI826 flagella, and analyzed using an SAv-coated biotin chip.

Fig. 6 reveals the selective recognition capability of the SAv chip over two different *E. coli* GI826 cells. The QCM detection system was run at a much slower flow rate than that used in immunoassays to avoid shearing of the flagella. When the chip was first flowed over with the vector-carrying cells, the frequency declined very slightly and slowly. Nevertheless, a pronounced frequency response was readily observed once the *Strep*-tag II-displaying cells, the ones carrying pStrepII, were subsequently injected. A follow-up rinsing with the working buffer did not result in any restoration of the frequency, suggesting the strong interaction between the surface-capturing SAv and the cell-displayed *Strep*-tag II peptide.

Furthermore, STEM image analysis was carried out to confirm the disparity of SAv binding between those two different cells. Because of strong hydrogen-bonding interactions between dextran molecules, the gold nanoparticles coated with dextran–biotin were highly clustered together into colossal clumps, as shown in Fig. 7B,

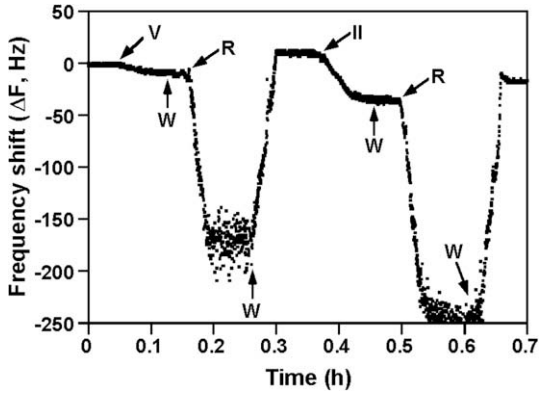

Fig. 6. Differential responses of an SAv chip toward different *E. coli* GI826 cells. SAv was adsorbed onto the biotin chip by the static immersion method. The descriptions of R and W are the same as those in Figs. 2 and 4. V, 0.5-ml cells carrying pFliTrx; II, 0.5-ml cells carrying pStrepII. Flow rate: 101 μl/min. Cell density: 5×10^8 CFU/ml.

which was distinctly different from the perfect segregation of alkanethiol-coated nanoparticles (Fig. 7A). The cell morphologies of *E. coli* GI826 cells were not visibly affected by the insertion of *Strep*-tag II (Figs. 7C and D) because the peptide contains only 10 amino acids. However, STEM examination of the mixtures of biotin-coated particles with the cells, which had been preincubated with SAv, revealed that only the cells expressing *Strep*-tag II had the capability to bind with SAv and consequently attract biotin nanoparticle clusters onto the cell surface (Fig. 7D). On the contrary, the vector-carrying cells lacked the SAv binding ability and were observed as separate entities from the nanoparticle clusters at all times (Fig. 7C). Therefore, the STEM results agreed well with those obtained using the QCM biosensor, suggesting that the SAv chip exhibited satisfactory differential ability to recognize *E. coli* cells expressing biotin-mimic peptides while also offering the advantages of direct detection, fast response, real-time output, and experimental simplicity over the STEM analysis.

QCM binding affinity of Strep-tag II-expressing cells

Finally, the binding kinetics of the *Strep*-tag II-expressing cells to the chip surface-coated SAv was studied. Due to the strong interaction and consequently the lack of a dissociation sensorgram in the real-time biosensor study, the direct estimation of kinetic parameters by fitting the sensorgrams could not be conducted. Therefore, equilibrium binding kinetics [3] was studied instead. A single SAv chip was used to continuously detect different concentrations of the *Strep*-tag II-displaying cells. To ensure the achievement of complete adsorption equilibrium, an excess amount of each cell solution was allowed to continuously pass over the crystal until a steady resonant frequency had been reached, followed by the rinsing with the working buffer and the acidic regeneration.

Fig. 8 shows the dependence on cell concentrations of the response equilibrium frequency shifts of that chip. The rectangular–hyperbolic relationship suggests that the adsorption of the cells can be illustrated by a Langmuir single-site binding isotherm using Eq. (3):

$$-\Delta F_e = \frac{-\Delta F_{e,max} C}{K_D + C}, \tag{3}$$

where $-\Delta F_{e,max}$ is the saturation equilibrium frequency shift when all the active binding sites on the SAv chip are occupied, C is the cell concentration, and K_D is the apparent dissociation constant. As shown in Fig. 8, the frequency shift data were satisfactorily fitted with Eq. (3) (correlation coefficient $R = 0.982$). Three duplicate anal-

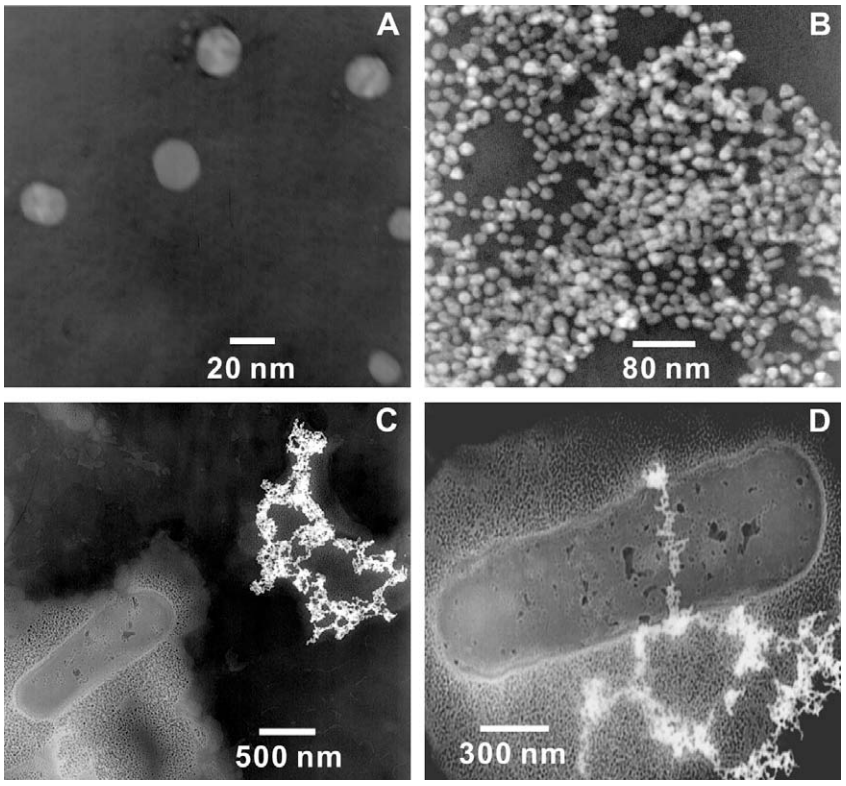

Fig. 7. STEM images. (A) 16-MA-coated gold nanoparticles. (B) Biotin-coated gold nanoparticles. (C, D) Mixtures of biotin-coated gold nanoparticles with SAv-treated *E. coli* GI826 cells carrying pFliTrx (C) and pStrepII (D), respectively. In panel C, a single cell (the brightly rimmed rod at the lower left corner) is distinctly separated from a cluster of nanoparticles (the bright-dotted clump at the upper right corner). In panel D, the cell is belted and attached by the particle clusters.

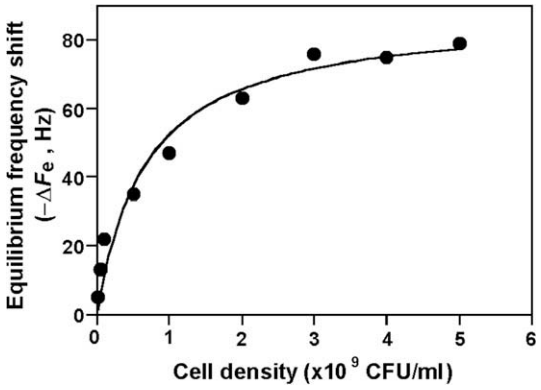

Fig. 8. Concentration effect of pStrepII-carrying cells on equilibrium frequency shifts of an SAv chip that was prepared by the static immersion method. The solid line was obtained by nonlinear fitting of the experimental data using Eq. (3).

yses, each using a single SAv chip, yielded averages of $6.8 \pm 1.9 \times 10^8$ CFU/ml and 88 ± 6 Hz, respectively, for the estimated K_D and $-\Delta F_{e,max}$ values. Furthermore, considering the typical estimate that there are approximately 330,000 copies of FliC protein, the major bacterial flagellin protein, on each natural *E. coli* cell (http://redpoll.pharmacy.ualberta.ca/CCDB/cgi-bin/STAT_NEW.cgi) and the fact that each FliC protein had been inserted with one copy of the *Strep*-tag II peptide, the K_D value between the surface-capturing SAv and the cell-displayed *Strep*-tag II peptide was estimated as 0.37 μM. However, a K_D value smaller than 0.37 μM is considered as a more appropriate estimate for the current study because a lower copy number of FliC protein would be expected for each recombinant cell due to the effects of plasmid stability and expression efficiency. Compared with the previously reported data of standalone synthetic *Strep*-tag II peptides interacting with free SAV using an isothermal titration calorimetry assay (72 μM) [24] and of flowing bBSA binding on a SAv-coated chip using a QCM biosensor (0.11–0.24 μM) [7], the current result is close to the latter value, implying that the cell-displayed peptides bound to the chip surface SAv in a way similar to that of the BSA-conjugated biotin.

Conclusions

We have presented a cost-effective and reliable preparation method for hydrogel-coated biotin QCM chips and demonstrated the effective applications of the chips for immunoassays of anti-BSA and selective analyses of *Strep*-tag II-displaying cells. The precoupling of the dextran–biotin complex permits better control of the chip fabrication process by monitoring its coupling efficiency. The gel complex solution can be used multiple times in the dip-coating process of modifying the alkanethiol-coated chips, reducing the expense of biotin derivatives. The immunoassay study demonstrates the feasibility of a highly efficient on-line coating method with a biotinylated antigen. The antibody-containing samples can be continuously and repetitively assayed with high selectivity and sensitivity using the same single chip. Such a combined process not only provides experimental convenience and efficiency but also increases assay sensitivity by eliminating the possibility of antigen denaturation that may occur during off-line coating. The good agreement of the results between the biosensor and STEM studies from two different peptide-displaying cells again shows the possibility of employing the prepared SAv chip to screen biotin-mimic peptides from a cell display random peptide library. Furthermore, the K_D value of the *Strep*-tag II-expressing cells binding to the chip surface-coated SAv was successfully estimated by equilibrium binding kinetics. This demonstrates that selectively screening peptides of high binding affinity from the peptide library directly by on-line estimation of kinetic parameters resolved by the prepared QCM biosensor is a promising application.

Acknowledgment

The research was supported by the National Science Council of the Republic of China.

References

[1] A.S. Hoffman, Hydrogel for biomedical applications, Adv. Drug Deliv. Rev. 54 (2002) 3–12.
[2] S. Löfås, B. Johnsson, A novel hydrogel matrix on gold surfaces in surface plasmon resonance sensors for fast and efficient covalent immobilization of ligands, J. Chem. Soc. Chem. Commun. 21 (1990) 1526–1528.
[3] H.-C. Lu, H.-M. Chen, Y.-S. Lin, J.-W. Lin, A reusable and specific protein A-coated piezoelectric biosensor for flow injection immunoassay, Biotechnol. Prog. 16 (2000) 116–124.
[4] H.-M. Chen, W.-C. Wang, S.-H. Chen, A metal-chelating piezoelectric sensor chip for direct detection and oriented immobilization of polyHis-tagged proteins, Biotechnol. Prog. 20 (2004) 1237–1244.
[5] J. Heo, R.M. Crooks, Microfluidic biosensor based on an array of hydrogel-entrapped enzymes, Anal. Chem. 77 (2005) 6843–6851.
[6] R.C.H. Kwan, P.Y.T. Hon, R. Renneberg, Amperometric determination of ammonium with bienzyme/poly(carbamoyl) sulfonate hydrogel-based biosensor, Sens. Actuat. B 107 (2005) 616–622.
[7] H.-M. Chen, C.-W. Lin, Hydrogel-coated streptavidin piezoelectric biosensors and applications to selective detection of Strep-tag displaying cells, Biotechnol. Prog. 23 (2007) 741–748.
[8] R.V. Ulijn, N. Bibi, V. Jayawarna, P.D. Thornton, S.J. Todd, R.J. Mart, A.M. Smith, J.E. Gough, Bioresponsive hydrogels, Mater. Today 10 (2007) 40–48.
[9] G.Z. Sauerbrey, Use of quartz vibrator for weighing thin films on a microbalance, Z. Phys. 155 (1959) 206–211.
[10] A. Hengerer, C. Kösslinger, J. Decker, S. Hauck, I. Queitsch, H. Wolf, S. Dübel, Determination of phage antibody affinities to antigen by a microbalance sensor system, BioTechniques 26 (1999) 956–964.
[11] A. Janshoff, H.-J. Galla, C. Steinem, Piezoelectric mass-sensing devices as biosensors: an alternative to optical biosensors?, Angew Chem. Intl. Ed. 39 (2000) 4004–4032.
[12] K.-I. Sano, K. Shiba, A hexapeptide motif that electrostatically binds to the surface of titanium, J. Am. Chem. Soc. 125 (2003) 14234–14235.
[13] S. Tombelli, M. Mascini, A.P.F. Turner, Improved procedures for immobilisation of oligonucleotides on gold-coated piezoelectric quartz crystals, Biosens. Bioelectron. 17 (2002) 929–936.
[14] H.-M. Chen, M.-L. Lin, S.-H. Chen, Fabrication of piezoelectric biochips with self-assembled alkanethiol layer and hydrocoating, J. Chin. Inst. Chem. Eng. 34 (2003) 151–160.
[15] J. Rickert, A. Brecht, W. Göpel, Quartz crystal microbalances for quantitative biosensing and characterizing protein multilayers, Biosens. Bioelectron. 12 (1997) 567–575.
[16] S. Storri, T. Santoni, M. Minunni, M. Mascini, Surface modifications for the development of piezoimmunosensors, Biosens. Bioelectron. 13 (1998) 347–357.
[17] H.-M. Chen, K.-T. Chen, Production and characterization of glutathione S-transferase fused with a metal chelating peptide, Enzyme Microb. Technol. 27 (2000) 219–226.
[18] N.M. Green, Avidin and streptavidin, Methods Enzymol. 184 (1990) 51–67.
[19] G.M. Sharma, K.H. Roux, S.K. Sathe, A sensitive and robust competitive enzyme-linked immunosorbent assay for Brazil nut (*Bertholletia excelsa* L.) detection, J. Agric. Food Chem. 57 (2009) 769–776.
[20] K.-Z. Liang, J.-S. Qi, W.-J. Mu, Z.-X. Liu, Conductometric immunoassay for interleukin-6 in human serum based on organic/inorganic hybrid membrane-functionalized interface, Bioproc. Biosyst. Eng. 32 (2009) 353–359.
[21] A. Kausaite, M. van Dijk, J. Castrop, A. Ramanaviciene, J.P. Baltrus, J. Acaite, A. Ramanavicius, Surface plasmon resonance label-free monitoring of antibody antigen interactions in real time, Biochem. Mol. Biol. Educ. 35 (2007) 57–63.
[22] S. Tsuzuki, A. Wada, Y. Ito, Photo-immobilization of biological components on gold-coated chips for measurements using surface plasmon resonance (SPR) and a quartz crystal microbalance (QCM), Biotechnol. Bioeng. 102 (2008) 700–707.
[23] Z. Lu, K.S. Murray, V.V. Cleave, E.R. LaVallie, M.L. Stahl, J.M. McCoy, Expression of thioredoxin random peptide libraries on the *Escherichia coli* cell surface as functional fusions to flagellin: a system designed for exploring protein–protein interactions, Biotechnology 13 (1995) 366–372.
[24] T.G.M. Schmidt, J. Koepke, R. Frank, A. Skerra, Molecular interaction between the Strep-tag affinity peptide and its cognate target, streptavidin, J. Mol. Biol. 255 (1996) 753–766.